International Journal of Civil Engineering and Technology (IJCIET)
Volume 8, Issue 2, February 2017, pp. 51–71 Article ID: IJCIET_08_02_007
Available online at http://www.iaeme.com/IJCIET/issues.asp?JType=IJCIET&VType=8&IType=2
ISSN Print: 0976-6308 and ISSN Online: 0976-6316

EXPERIMENTAL VERIFICATION OF MULTIPLE CORRELATIONS BETWEEN THE SOIL YOUNG MODULUS AND THEIR IDENTIFICATION PARAMETERS

Messi Alfred François, Mamba Mpele, Tchoumi Dany Franky
Department of Civil Engineering, National Advanced School of Engineering,
University of Yaounde I, P.O. Box 8390, Cameroon.

Koumbe Mbock
African Center of Excellence in Information and Communication Technologies,
University of Yaounde I, Cameroon.

Ndom Francis Rollins
Department of Mathematics and Physics, National Advanced School of Engineering,
University of Yaounde I, Cameroon.

Befere Godlove
National Civil Engineering Laboratory of Cameroon

ABSTRACT

This paper consists to verify the validation of two multiple correlations between the Young's modulus (E) of a soil and its identification parameters. These correlations are used to calculate two types of theoretical moduli called E_{SIKALI} and E_{LCPC}. The exploitation of triaxial test results allows specifying 4 experimental moduli such as the initial modulus E_t^0, the equivalent modulus E_{elq}, the secant modulus at 1/2 and 1/3 of the breaking strain $Esec_{1/2}$ and $Esec_{1/3}$. Our approach compares the theoretical and experimental modulus through straight linear regressions. The results show that the E_{LCPC} better represents E_t^0 and E_{elq} while the E_{SIKALI} is more consistent with $Esec_{1/2}$.

Key words: Multiple correlations, Linear regressions, Experimental and Theoritical Young modulus and Identification parameters

Cite this Article: Messi Alfred François, Mamba Mpele, Tchoumi Dany Franky, Koumbe Mbock, Ndom Francis Rollins and Befere Godlove, Experimental Verification of Multiple Correlations Between the Soil Young Modulus and their Identification Parameters. *International Journal of Civil Engineering and Technology*, 8(2), 2017, pp. 51–71.
http://www.iaeme.com/IJCIET/issues.asp?JType=IJCIET&VType=8&IType=2

1. INTRODUCTION

A joint study from the National Advanced School of Engineering (ENSP) and the National Civil Engineering Laboratory of Cameroon (LABOGENIE) has established multiple correlations between the Young's modulus (E) and the parameters of identification of lateritic soils [13, 15, 22]. However, the Young's moduli involved in the procedure has not been determined experimentally but deduced from empirical formulas. There are several different Young's moduli, but empirical formulas proposed in the literature [20, 21] do not specify if the estimated E isinitial, equivalent or secant.

This paper consists to verify the validation of those multiple correlations through experimental tests. For this purpose, the Young's modulus is determined by adopting as soil behavior law hyperbolic model of Wong and Duncan. To obtain more specifications on the nature of the estimated Young's moduli, the present study makes use of 26 samples of lateritic soils and the results are presented in order to show that the E_{LCPC} better represents E_t^0 and E_{elq} while the E_{SIKALI} is more consistent with $Esec_{1/2}$.

In this section, we introduce our work and section 2 deals with the materials and the experimental procedure of our approach. In this section we develop methodology that aims to verify the multiple correlations. The section III presents the different results and we conclude this study in section 4 with a short discussion.

2. MATERIALS AND EXPERIMENTAL PROCEDURES

To develop the methodology of our approach, we define the parameters of the multiple correlation model given in table 1 below:

Table 1 Model parameters

Parameter	Description	Mean of finding
D_{max}	Maximum diameter of soil particles	Sieve and hydrometer analysis [NF P94-056. NF P94-057]
P_{80}	Percent finer than 80 µm by weight	
D_{50}	Diameter of the particle at 50 percent finer on the grain size distribution curve	
G	Percent by weight of particles coarser than 2 mm and finer than 20 mm	
S	Percentby weight of particles coarser than 20 µm and finer than 2 mm	
L	Percent by weight of particles coarser than 2 µm and finer than 20 µm	
A	Percent by weight of particles finer than 2 µm	
PI	Plasticity Index	Atterberg limits tests [NF P 94-051. NF P 94-052]
E_{LCPC}	Young modulus determined by the LCPC formula	E_{LCPC} = 5 CBR (E in MPa) [20]
E_{SIKALI}	Young modulus determined by the SIKALI-MUNDI formula	$E_{SIKALI}(E\ in\ bars) = \begin{cases} 19CBR\ if\ P80 < 35\% \\ 17CBR\ if\ P80 > 35\% \end{cases}$ [21]

The correlation models to be verified in this study are given in the table 2:

Table 2 Correlation equations in [22]

N°	Power models
1	$E_{LCPC} = D_{max}^{0.94901} PI^{-0.32725} D_{50}^{0.07986} G^{0.56787} S^{0.45942} L^{0.13219} A^{-0.29770}$
2	$E_{SIKALI} = D_{max}^{0.79900} PI^{-0.36328} D_{50}^{0.09940} G^{0.53986} S^{0.39927} L^{0.10129} A^{-0.18852}$

The procedure consists to compare the calculated and the experimental values of the Young modulus. In one side, by using the results of soil identification, the calculated value of E is determined with the formulas of the table 2. In the other side, the results of the triaxial test give the stress and strain values of the hyperbolic model of Duncan and Wong in order to find the experimental values of E. We examine four types of moduli, namely,the initial tangent modulus E_t^0, the equivalent elastic modulus E_{elq}, the secant moduli at half the breaking strain $Esec_{1/2}$ and the secant modulus at one third of the breaking strain $Esec_{1/3}$.

2.1. The hyperbolic model of DUNCAN and WONG

In this model, the soil behavior law is based on an approximation stress-strain behavior of curves obtained by a drained compression triaxial test. The hyperbolic approach is the basis of Duncan and Wong model; the experimental curve $[(\sigma_1 - \sigma_3), \varepsilon_1]$ is approximated by the hyperbola of the equation:

$$(\sigma_1 - \sigma_3) = \frac{\varepsilon_1}{a + b\varepsilon_1} \quad (1)$$

where σ_3, $(\sigma_1 - \sigma_3)$ and ε_1 are respectively the hydrostatic pressure, the axial stress and the vertical strain. The constants a and b depend on the triaxial test.

The expression $\left[\frac{d(\sigma_1-\sigma_3)}{d\varepsilon_1}\right]_i = E_t^i$ is obtained by deriving the hyperbolic curve at the point with coordinate $[\varepsilon_1^i, (\sigma_1 - \sigma_3)_i]$. This is also the slope of the tangent or the increment of the Young's tangent modulus at this point.

We have

$$\frac{d(\sigma_1-\sigma_3)}{d\varepsilon_1} = \frac{a}{(a+b\varepsilon_1)^2} = E_t \begin{cases} for\ \ \varepsilon_1 = \varepsilon_1^i \\ E_t = E_t^i \end{cases} \quad (2)$$

So E_t^0 correspond to $\varepsilon_1 = 0$; E_t^0 is the initial tangent modulus. Then, we have

$$E_t^0 = \frac{1}{a} \quad (3)$$

If we let $(\sigma_1 - \sigma_3)_{ult} = \lim_{\varepsilon_1 \to \infty} \left[\frac{\varepsilon_1}{a+b\varepsilon_1}\right] = \frac{1}{b}$ and the ultimate is denoted by the index ult , the hyperboliclawis translated as:

$$(\sigma_1 - \sigma_3) = \frac{\varepsilon_1}{\frac{1}{E_t^0} + \frac{\varepsilon_1}{(\sigma_1-\sigma_3)_{ult}}} \quad (4)$$

We can also write:

$$E_t = E_t^0 \left[1 - \frac{\sigma_1-\sigma_3}{(\sigma_1-\sigma_3)_{ult}}\right]^2 \quad (5)$$

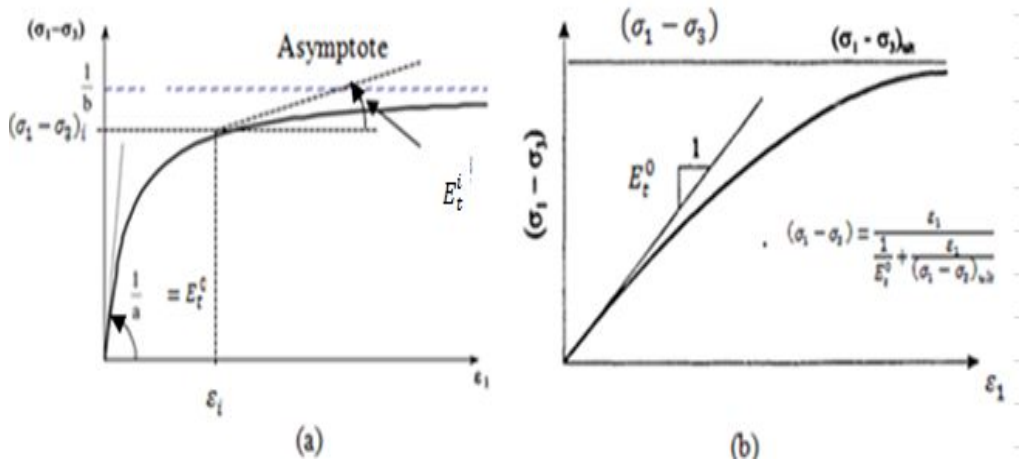

Figure 1 Hyperbolic law: (a) represents E_t^0 and E_t^i, (b) represents the law itself

Wong and Duncan also propose to choose a point in the vicinity of the ultimate stress (asymptote) and set this point as breaking point; we then define a parameter R_f such that :

$$R_f = \frac{(\sigma_1-\sigma_3)_{rupt}}{(\sigma_1-\sigma_3)_{ult}} \tag{6}$$

where the breaking is denoted by the index rupt and the ultimate is by the index ult. .

Let C' be the soil cohesion stress and $\varphi'$the angle of internal friction of soil under effective stress. The breaking point is also supposed to verify the Mohr-Coulomb criteria:

$$(\sigma_1-\sigma_3)_{rupt} = \frac{2C\prime\cos\varphi\prime+2\sigma_3'\sin\varphi\prime}{1-\sin\varphi\prime} \tag{7}$$

We will have

$$(\sigma_1-\sigma_3)_{ult} = \frac{(\sigma_1-\sigma_3)_{rupt}}{R_f} = \frac{2C'\cos\varphi'+2\sigma_3'\sin\varphi'}{R_f[1-\sin\varphi']} \tag{8}$$

And

$$E_t = E_t^0\left[1-\frac{R_f(1-\sin\varphi')(\sigma_1-\sigma_3)}{2C'\cos\varphi'+2\sigma_3'\sin\varphi'}\right] \tag{9}$$

It is often more convenient to effect a transformation of the hyperbolic pattern in linear diagram according to the following formulation:

$$\frac{\varepsilon_1}{\sigma_1-\sigma_3} = \frac{1}{E_t^0} + \frac{\varepsilon_1}{(\sigma_1-\sigma_3)_{ult}} \tag{10}$$

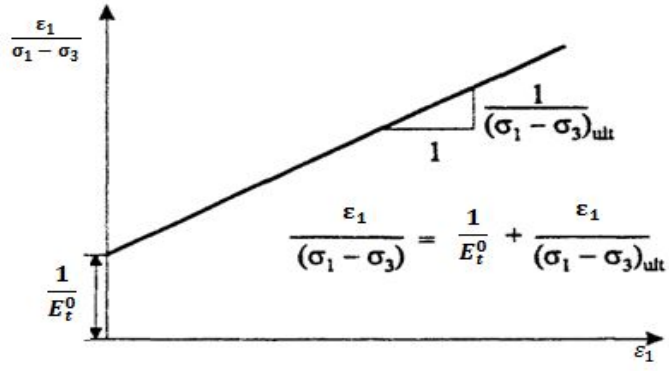

Figure 2 Linear representation of the hyperbolic law of Wong and Duncan [13]

The experience gained by Duncan and other mechanics of soil by performing simulations of stress-strain curves for different soils, showed that after the carrying of point of measurement onto the transformed linear diagram, these points are sometimes quite far from a perfect alignment. Thus a higher or lower concavity as far as the soil is dense or loose, is observed.

2.2. Expression of experimental E based on Wong and Duncan model

2.2.1. Expression of E_t^0 and E_t

According to Wong and Duncan [13], good setting can be obtained with the line:

$$\frac{\varepsilon_1}{\sigma_1-\sigma_3} = f(\varepsilon_1) \tag{11}$$

Passing through the two points corresponding respectively to 70% and 95% of the tensile strength $(\sigma_1 - \sigma_3)_{\text{rupt}}$. In practice, these two points are carried into the transformed plane and is enough to define the right of transformation.

The slope of this line is then given by:

$$\frac{1}{(\sigma_1-\sigma_3)_{ult}} = \left(\frac{\varepsilon_1^{95\%}}{(\sigma_1-\sigma_3)_{rupt}^{95\%}} - \frac{\varepsilon_1^{70\%}}{(\sigma_1-\sigma_3)_{rupt}^{70\%}}\right)\frac{1}{\varepsilon_1^{95\%}-\varepsilon_1^{70\%}}$$

$$= \frac{1}{0.665(\sigma_1-\sigma_3)_{rupt}}\left(\frac{0.70\varepsilon^{95\%}-0.95\varepsilon_1^{70\%}}{\varepsilon_1^{95\%}-\varepsilon_1^{70\%}}\right) \tag{12}$$

where $\varepsilon_1^{95\%}$and $\varepsilon_1^{70\%}$ are respectively strain at 95% and 70% of breaking.

We deduce

$$\frac{1}{E_t^0} = \left[\frac{\varepsilon_1^{70\%}\varepsilon_1^{95\%}}{\varepsilon_1^{95\%}-\varepsilon_1^{70\%}}\right]\left[\frac{1}{(\sigma_1-\sigma_3)_{rupt}^{70\%}} - \frac{1}{(\sigma_1-\sigma_3)_{rupt}^{95\%}}\right] \tag{13}$$

Then

$$\frac{1}{E_t^0} = \frac{1}{2.66(\sigma_1-\sigma_3)_{rupt}}\left(\frac{\varepsilon_1^{70\%}\varepsilon_1^{95\%}}{\varepsilon_1^{95\%}-\varepsilon_1^{70\%}}\right) \tag{14}$$

From the expressions

$$E_t = E_t^0\left[1 - \frac{\sigma_1-\sigma_3}{(\sigma_1-\sigma_3)_{ult}}\right]^2 \tag{15}$$

and

$$(\sigma_1-\sigma_3)_{ult} = \frac{(\sigma_1-\sigma_3)_{rupt}}{R_f} = \frac{2C'\cos\varphi\prime+2\sigma_3\sin\varphi\prime}{R_f(1-\sin\varphi\prime)} \tag{14}$$

we obtain:

$$E_t = E_t^0\left[1 - \frac{R_f(1-\sin\varphi')[\sigma_1-\sigma_3]}{2C'\cos\varphi'+2\sigma_3\sin\varphi'}\right]^2 \tag{17}$$

2.2.2. The equivalent linear elastic modulus E_{elq}

The moduli are assumed reversible in the elastic area whether linear or non-linear. Consider respectively linear elastic law (Hooke's law) and the hyperbolic elastic law. ε_{el} denotes the linear elastic strain limit and ε_{eh}, hyperbolic limits strainand $(\sigma_1-\sigma_3)_{el}$ and $(\sigma_1-\sigma_3)_{eh}$ the corresponding stresses.

As presented in figure 3a below for $\varepsilon_1^i \leq \varepsilon_{el}$, we have the linear elastic law:

$$(\sigma_1 - \sigma_3)_e^i = E_{el} \tag{18}$$

In figure 3b for$\varepsilon_1^i \leq \varepsilon_{eh}$, we also have the hyperbolic law:

$$(\sigma_1 - \sigma_3)_h^i = \frac{\varepsilon_1^i}{\frac{1}{E_t^0} + \frac{\varepsilon_1^i}{(\sigma_1 - \sigma_3)_{ult}}} \tag{19}$$

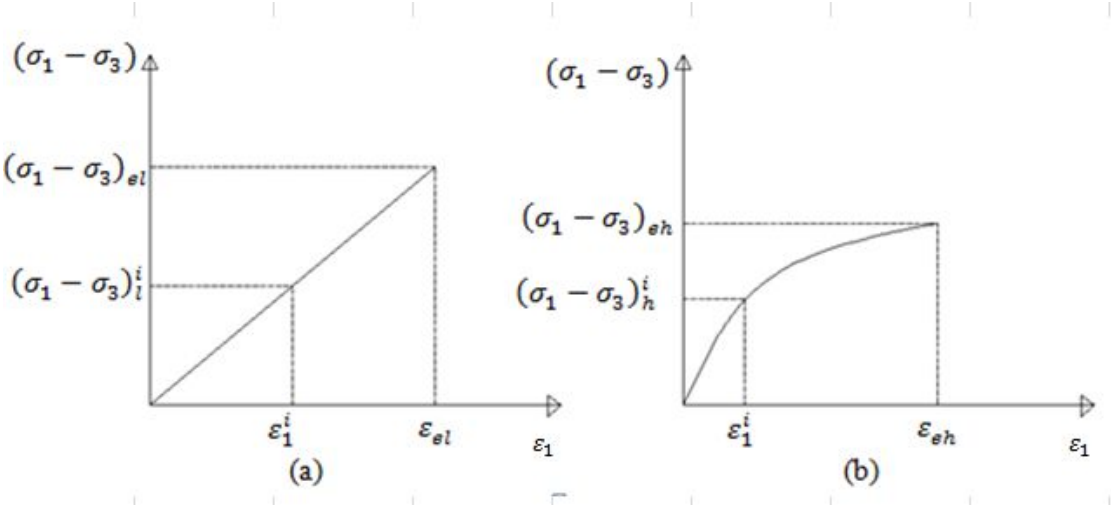

Figure 3 Accent of the laws: (a) Linear elastic law and (b) hyperbolic law

If one equates the hyperbolic law to Hooke's law we will obtain

$$(\sigma_1 - \sigma_3)_{he}^i = E_{elq}\varepsilon_1^i \tag{20}$$

With E_{elq}, being the equivalent linear elastic modulus and $(\sigma_1 - \sigma_3)_{he}^i$ hyperbolic stress equivalent to the linear stress.

$\Delta(\sigma_1 - \sigma_3)^i$, the error committed in equating the hyperbolic law to the linear law.

$$\begin{aligned}\Delta(\sigma_1 - \sigma_3)^i &= (\sigma_1 - \sigma_3)_h^i - (\sigma_1 - \sigma_3)_{he}^i \\ &= (\sigma_1 - \sigma_3)_h^i - E_{elq}\varepsilon_1^i\end{aligned} \tag{21}$$

The residual variation

$$S\left[\Delta(\sigma_1 - \sigma_3)^i\right] = \sum_{i=1}^{N}\left[(\sigma_1 - \sigma_3)_h^i - E_{elq}\varepsilon_1^i\right]^2$$

$$S\left[\Delta(\sigma_1 - \sigma_3)^i\right] = \sum_{i=1}^{N}\left[\left[(\sigma_1 - \sigma_3)_h^i\right]^2 - 2E_{elq}\varepsilon_1^i(\sigma_1 - \sigma_3)_h^i + E_{elq}^2\left(\varepsilon_1^i\right)^2\right] \tag{22}$$

To find the value of E_{elq} which minimize the error :

$$\frac{dS\left[\Delta(\sigma_1 - \sigma_3)^i\right]}{dE_{elq}} = 0 \tag{23}$$

We have

$$\sum_{i=1}^{N}\left[-2\varepsilon_1^i(\sigma_1 - \sigma_3)_h^i + 2E_{elq}\left(\varepsilon_1^i\right)^2\right] = 0 \tag{23}$$

$$E_{elq} = \frac{\sum_{i=1}^{N} \varepsilon_1^i (\sigma_1 - \sigma_3)_h^i}{\sum_{i=1}^{N} (\varepsilon_1^i)^2} \quad (24)$$

With $\varepsilon_{1i} \leq \varepsilon_{eh}$

The expression of the incertainty on $E_{elq.}$This method is experimental, it occurs during testing difficulties affecting the measurement results:

- The sudden closing of cracks at the beginning of change;
- The friction of the piston ;
- The imperfect sample size.

The uncertainty in the determination of Young's modulus is then determined by differentiation of the natural logarithm applied to the expression of E_{elq} :

$$\ln E_{elq} = \ln\left[\frac{\sum_{i=1}^{N} (\sigma_1 - \sigma_3)_h^i \varepsilon_1^i}{\sum_{i=1}^{N} (\varepsilon_1^i)^2}\right] = \ln\left[\sum_{i=1}^{N} (\sigma_1 - \sigma_3)_h^i \varepsilon_1^i\right] - \ln[\sum_{i=1}^{N} (\varepsilon_1^i)^2]$$

$$\frac{dE_{elq}}{E_{elq}} = \frac{d[\sum_{i=1}^{N} (\sigma_1 - \sigma_3)_h^i \varepsilon_1^i]}{\sum_{i=1}^{N} (\sigma_1 - \sigma_3)_h^i \varepsilon_1^i} - \frac{d\left[\sum_{i=1}^{N} (\varepsilon_1^i)^2\right]}{\sum_{i=1}^{N} (\varepsilon_1^i)^2}$$

$$= \frac{\sum_{i=1}^{N} [d(\sigma_1 - \sigma_3)_h^i \varepsilon_1^i + (\sigma_1 - \sigma_3)_h^i d\varepsilon_1^i]}{\sum_{i=1}^{N} (\sigma_1 - \sigma_3)_h^i \varepsilon_1^i} - \frac{\sum_{i=1}^{N} 2\varepsilon_1^i d\varepsilon_1^i}{\sum_{i=1}^{N} (\varepsilon_1^i)^2}$$

$$\frac{\Delta E_{elq}}{E_{elq}} = \frac{\sum_{i=1}^{N} [\Delta(\sigma_1 - \sigma_3)_h^i \varepsilon_1^i + (\sigma_1 - \sigma_3)_h^i \Delta\varepsilon_1^i]}{\sum_{i=1}^{N} (\sigma_1 - \sigma_3)_h^i \varepsilon_1^i} - \frac{\sum_{i=1}^{N} 2\varepsilon_1^i \Delta\varepsilon_1^i}{\sum_{i=1}^{N} (\varepsilon_1^i)^2} \quad (25)$$

Taking $\Delta[(\sigma_1 - \sigma_3)_h^i] = 2\Delta\sigma$ and replacing in (25) , we have :

$$\frac{\Delta E_{elq}}{E_{elq}} = \frac{\sum_{i=1}^{N} [2\Delta\sigma\varepsilon_1^i + (\sigma_1 - \sigma_3)_h^i \Delta\varepsilon_1^i]}{\sum_{i=1}^{N} (\sigma_1 - \sigma_3)_h^i \varepsilon_1^i} - \frac{\sum_{i=1}^{N} 2\varepsilon_1^i \Delta\varepsilon_1^i}{\sum_{i=1}^{N} (\varepsilon_1^i)^2} \quad (26)$$

Supposing $\Delta\varepsilon_1^i$ constant, (26) is rewritten as :

$$\frac{\Delta E_{elq}}{E_{elq}} = \frac{2\Delta\sigma \sum_{i=1}^{N} \varepsilon_1^i}{\sum_{i=1}^{N} (\sigma_1 - \sigma_3)_h^i \varepsilon_1^i} + \frac{\Delta\varepsilon_1^i \sum_{j=1}^{N} (\sigma_1 - \sigma_3)_h^j}{\sum_{i=1}^{N} (\sigma_1 - \sigma_3)_h^i \varepsilon_1^i} + \frac{2\Delta\varepsilon_1^i \sum_{j=1}^{N} \varepsilon_1^j}{\sum_{i=1}^{N} (\varepsilon_1^i)^2} \quad (27)$$

Knowing that $(\sigma_1 - \sigma_3)_h^i \leq (\sigma_1 - \sigma_3)_{eh}and\varepsilon_1^i \leq \varepsilon_{eh}$, we have

$$\sum_{i=1}^{N} (\sigma_1 - \sigma_3)_h^i \varepsilon_1^i \leq (\sigma_1 - \sigma_3)_{eh} \sum_{i=1}^{N} \varepsilon_1^i \quad (28)$$

Considering $\sum_{i=1}^{N} (\sigma_1 - \sigma_3)_h^i \varepsilon_1^i \leq \varepsilon_{eh} \sum_{i=1}^{N} (\sigma_1 - \sigma_3)_h^i$and $\sum_{i=1}^{N} (\varepsilon_1^i)^2 \leq \varepsilon_{eh} \sum_{i=1}^{N} \varepsilon_1^i$, we will also have

$$\frac{2\Delta\sigma \sum_{i=1}^{N} \varepsilon_1^i}{\sum_{i=1}^{N} (\sigma_1 - \sigma_3)_h^i \varepsilon_1^i} \geq \frac{2\Delta\sigma}{(\sigma_1 - \sigma_3)_{eh}} \quad (29)$$

Then

$$\frac{\Delta\varepsilon_1^i \sum_{i=1}^{N} (\sigma_1 - \sigma_3)_h^i}{\sum_{i=1}^{N} (\sigma_1 - \sigma_3)_h^i \varepsilon_1^i} \geq \frac{\Delta\varepsilon_1^i}{\varepsilon_{eh}} \quad (30)$$

and

$$\frac{2\Delta\varepsilon_1^i \sum_{j=1}^{N} \varepsilon_1^j}{\sum_{i=1}^{N}\left(\varepsilon_1^i\right)^2} \geq \frac{2\Delta\varepsilon_1^i}{\varepsilon_{eh}} \tag{31}$$

where

$$\frac{\Delta E_{elq}}{E_{elq}} \geq \frac{3\Delta\varepsilon_1^i}{\varepsilon_{eh}} + \frac{2\Delta\sigma}{(\sigma_1-\sigma_3)_{eh}}$$

We consider the expression of ε_{1eh} et $(\sigma_1-\sigma_3)_{eh}$. The elasticity condition is given by the formula $f\left[(\sigma_1-\sigma_3)_h^i\right] \leq 0$ where $f[(\sigma_1-\sigma_3)_h^i]$ is the load function limiting the elastic range.

$$f\left[(\sigma_1-\sigma_3)_h^i\right] = (\sigma_1-\sigma_3)_h^i - (\sigma_1+\sigma_3)_h^i \sin\varphi' - 2C'^{\cos\varphi'} \tag{32}$$

We will have at the limit of the elastic range:

$$(\sigma_1-\sigma_3)_{eh} - (\sigma_1+\sigma_3)_{eh} \sin\varphi' - 2C'\cos\varphi' = 0$$

$$(\sigma_1-\sigma_3)_{eh} = \frac{2[C'\cos\varphi' + \sigma_{3eh}\sin\varphi']}{1-\sin\varphi'} \tag{33}$$

But we know that

$$(\sigma_1-\sigma_3)_{eh} = \frac{\varepsilon_{eh}}{\frac{1}{E_t^0} + \frac{\varepsilon_{eh}}{(\sigma_1-\sigma_3)_{ult}}} \tag{34}$$

Hence

$$\varepsilon_{eh} = \frac{(\sigma_1-\sigma_3)_{eh}}{E_t^0\left[1-\frac{(\sigma_1-\sigma_3)_{eh}}{(\sigma_1-\sigma_3)_{ult}}\right]} \tag{35}$$

2.2.3. Expression of $E_{sec1/3}$ and $E_{sec1/2}$

Generally, $E_{sec1/2}$, secant modulus corresponds to deviator $\frac{q_f}{2}$ by writing :

$$\frac{\varepsilon_{50}}{(\sigma_1-\sigma_3)} = \frac{1}{(\sigma_1-\sigma_3)_{ult}}\varepsilon_{50} + \frac{1}{E_t^0} \tag{36}$$

It therefore comes as:

$$E_{sec1/2} = E_t^0\left(1-\frac{R_f}{2}\right) \tag{37}$$

It is the same as $E_{sec1/3} = E_t^0\left(1-\frac{R_f}{3}\right)$

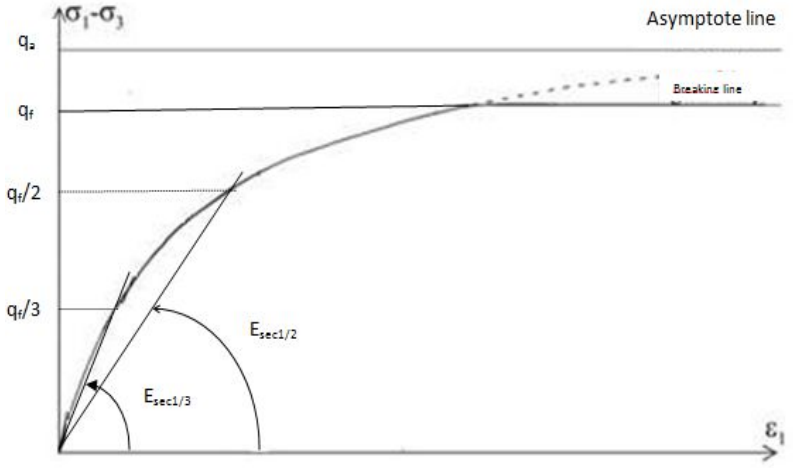

Figure4. Representation of Esec1/2 and Esec1/3

($q_f = (\sigma_1 - \sigma_3)_{rupt}$ et $q_a = (\sigma_1 - \sigma_3)_{ult}$)

2.3. Experimental Determination of Parameters

2.3.1. Presentation of Parameters to be Determined

By modeling the law of behavior of lateric soils using the hyperbolic laws of Wong and Duncan, the determination of Young Modulus and their uncertainty necessitates the measurement or the knowledge of the following parameters for every test j :

- The hydrostatic pressure σ_{3j}
- The axial stress or deviator $(\sigma_1 - \sigma_3)_j$
- The vertical deformation ε_{1j}
- The soil cohesion effective stress C'
- The angle of internal friction of the soil under effective stress φ'
- The deformation at 95% of breaking $\varepsilon_1^{95\%}$
- The deformation at 70% of breaking $\varepsilon_1^{70\%}$
- The deviator at 95% of breaking $95\%(\sigma_1 - \sigma_3)_{rupt}$
- The deviator at 70% of breaking $70\%(\sigma_1 - \sigma_3)_{rupt}$
- Coefficient Rf
- The hydrostatic pressure in the hyperbolic yield σ_{3eh}

2.3.2. Basic Information

The experimental determination of the parameters was carried out mainly on the basis of triaxial test results by LABOGENIE of 26 soil samples including 11 samples from Bini A Warak site and 15 samples of LOM PANGAR site. The device used is of the "Stady" mark in Figure 5.

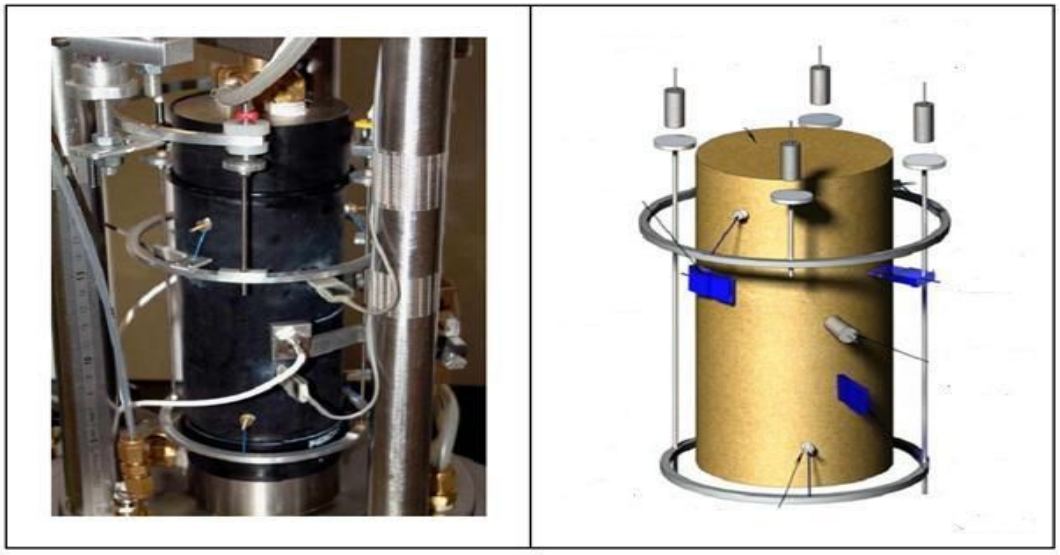

Figure 5 Photograph of a sample instrumented left and schematic view of the statistical measurement system (local) and dynamic (radial)

The principle of triaxial test consists of a cylindrical test sample a certain number of loading cycle which are the resultant of lateral pressure or confining variable σ_3 pressure and axial stress σ_1 equally variable. Displacement sensors allows for the measurement of the axial deformation (ε_1) (Figure 6).

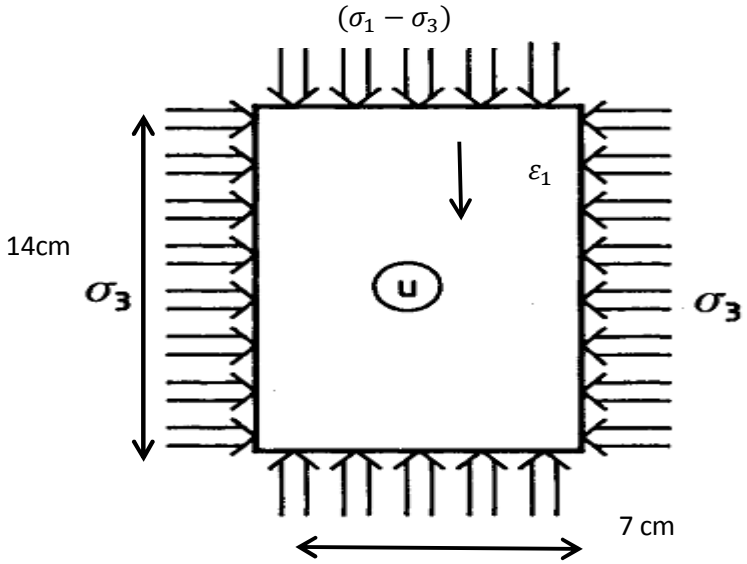

Figure 6 Representation of pressures applied to a test piece of the triaxial test

In practical terms, we fixed σ_3 and gradually increase σ_1 until rupture of the specimen. This will permit us to draw for a given value of σ_3 the curve $(\sigma_1 - \sigma_3) = f(\varepsilon_1)$. Tests in LABOGENIE were performed with three values of σ_3 (100kPa, 200kPa and 300kPa). Thus, each soil sample is characterized by three stress-strain curves. Figure 7 shows the representive curves of the sample N°5 fromBini A Warak site

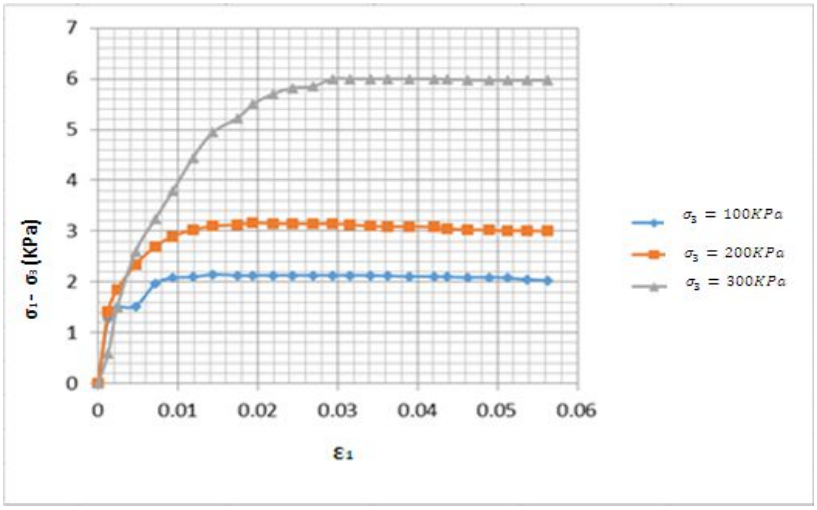

Figure 7 Representatives curves $(\sigma_1 - \sigma_3) = f(\varepsilon_1)$ of the sample N°5 from the Bini A Warak site

2.3.3. Determination of parameters C' and φ'

They are the parameters of elastic-plastic model of Mohr-Coulomb and these are determined at the end of the triaxial test. Thus, after drawing the stress-strain curve, we take for each level of confining stress, the maximum value of the stress deviator (effective stress). Then we place the point of abscissa $t = \frac{\sigma'_1 - \sigma'_3}{2}$ and $s = \frac{\sigma'_1 + \sigma'_3}{2}$ in lamé plan (s, t). Hence we get 3 points in the plane corresponding to each level of confinement. Using the linear regression method, we introduced a line called regression line, ensuring that the gap between the line and the various points is minimal.

We know that in the elastic range, we have:

$$\frac{\sigma'_1 - \sigma'_3}{2} = \frac{\sigma'_1 + \sigma'_3}{2} \sin\varphi' + C' \cos\varphi' \qquad (38)$$

which is a line ($y = ax + b$) in the Lame plan

Therefore by identification, we have:

- The slope is $a = \sin\varphi'$
- The intercept is : $b = C' \cos\varphi'$

We have realized for the sample N°6 of Bini A Warak site the calculation of the parameters and the next figure below presents the results obtained:

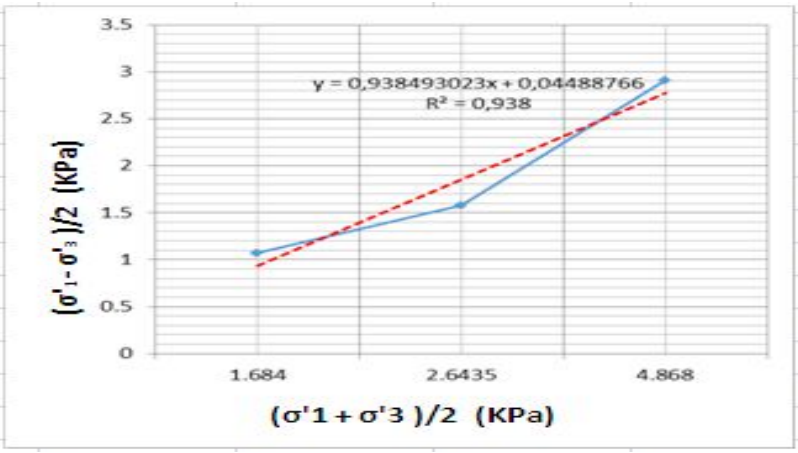

Figure 8 Regression line corresponding to the sample N°6 of the Bini AWarak site

Using the regression line, we get the parameters as it follows:

$$\sin\varphi' = 0.938493023 \Longrightarrow \varphi' = 34.9$$

$$C'\cos\varphi' = 0.4488766 \Longrightarrow C' = \frac{0.4488766}{\cos\varphi'} = 13kPa$$

The procedure is applied to all 26 samples and the results are presented in the following paragraph.

2.3.4. Determination of parameters $95\%(\sigma_1-\sigma_3)_{rupt}$, $70\%(\sigma_1-\sigma_3)_{rupt}$, $\varepsilon_1^{70\%}$, $\varepsilon_1^{95\%}$, Rf, *and* σ_{3eh},

The value of the deviator stress at breaking point is the maximum value of deviator. It is therefore trivial to calculate the values of $95\%(\sigma_1-\sigma_3)_{\text{rupt}}$and of $70\%(\sigma_1-\sigma_3)_{\text{rupt}}$. In regards to $\varepsilon_1^{70\%}$ and $\varepsilon_1^{95\%}$, using linear interpolation with two points flanking points respectively the points$[95\%(\sigma_1-\sigma_3)_{\text{rupt}};\ \varepsilon_{1\,95\%}]$ and $[70\%(\sigma_1-\sigma_3)_{\text{rupt}};\varepsilon_1^{70\%}]$ one can readily determine the parameters $\varepsilon_1^{70\%}$ and $\varepsilon_1^{95\%}$. These 4 parameters allow us to determine the value of the ultimate stress:

$$\frac{1}{(\sigma_1-\sigma_3)_{ult}} = \frac{1}{0.665(\sigma_1-\sigma_3)_{rupt}}\left(\frac{0.70\varepsilon_1^{95\%}-0.95\varepsilon_1^{70\%}}{\varepsilon_1^{95\%}-\varepsilon_1^{70\%}}\right) \quad (39)$$

As well as

$$\frac{1}{E_t^0} = \frac{1}{2.66(\sigma_1-\sigma_3)_{rupt}}\left(\frac{\varepsilon_1^{70\%}\varepsilon_1^{95\%}}{\varepsilon_1^{95\%}-\varepsilon_1^{70\%}}\right) \quad (40)$$

The parameter Rf is the ratio between the breaking deviator and the ultimate deviator. To simplify the calculations, we used Excel software to get the results from the N°1 sample from Bini A Warak site [table 3]:

Table 3 Parameters of the model of sample N°1

Stress				**Strain**		**Initial secant modulus**	**Ultimate stress**	**Coefficient**
σ_3 (kPa)	$(\sigma_1-\sigma_3)_{rupt}$ (kPa)	$(\sigma_1-\sigma_3)_{95\%}$ (kPa)	$(\sigma_1-\sigma_3)_{70\%}$ (kPa)	$\varepsilon_1^{95\%}$	$\varepsilon_1^{70\%}$	E_t^0(kPa)	$(\sigma 1-\sigma 3)_{ult}$ (kPa)	R_f
100	157.4	149.53	110.18	0.0041	0.0011	266471.35	172.87	0.9104
200	294.4	279.68	206.08	0.0093	0.0048	77223.283	455.05	0.6469
300	296.6	281.77	207.62	0.0125	0.0039	138664.26	336.26	0.8820

In the triaxial testing, soil is under 3 containment pressure levels. Each of these values correspond to parameter σ_{3eh}. We determine the parameter E_{elq}.

2.3.5. Determination of E_{elq}

The formula to estimate Young's modulus and its uncertainty involving the term

$$E_{elq} = \frac{\sum_{i=1}^{N}\varepsilon_1^i(\sigma_1-\sigma_3)_h^i}{\sum_{i=1}^{N}\left(\varepsilon_1^i\right)^2} \quad (41)$$

To determine the range of elasticity, we will do calculations on the N°1 sample and apply it to all other samples.

For $\sigma_3 = 100kPa$

$$(\sigma_1 - \sigma_3)_{eh} = \left(\frac{2 \cdot [0.23 \cdot cos(27.1) + 0.54 \cdot sin(27.1)]}{[1 - cos(27.1)]}\right) \times 100\ kPa$$

$$(\sigma_1 - \sigma_3)_{eh} = 161{,}22kPa$$

The range of elasticity is given by the formula:

$$\varepsilon_{eh} = \frac{(\sigma_1 - \sigma_3)_{eh}}{E_t^0\left[1 - \frac{(\sigma_1 - \sigma_3)_{eh}}{(\sigma_1 - \sigma_3)_{ult}}\right]} = \frac{161{,}22}{266471{,}352\left(1 - \frac{161{,}22}{229{,}523}\right)} = 0{,}0020$$

After having determined the three values of Young's modulus at different confinement pressures, the value retained for a sample will be the average of the three. Calculations performed on our No. 1 sample are presented in Table 4:

Table 4 Estimation of Young's modulus values for the BINI A WARAK site (Sample N°1)

$\sigma_3(kPa)$	ε_{eh}	E_{elqi} (KPa)	$\left\|\frac{\Delta E_{elq}}{E_{elq}}\right\|$	$\|\Delta E_{elq}\|(kPa)$	$E_{elq}(MPa)$
100	0.0020	77223.2837	0.0329	879.1277	171.45
200	0.0028	171847.318	0.1138		
300	0.00125	266471.352	0.0633		

2.3.6. Determination of parameters $E_{sec1/2}$ and $E_{sec1/3}$

Both parameters were calculated using formulas presented in paragraph 2.2.3. Table 5 presents the results of calculation performed on the sample N°1 (BINI A WARAK).

Table 5 Young's moduli values calculated on the BINI A WARAK samples (sample N°1)

E_t^0(Kpa)	Rf	$E_{sec1/2}$ (Kpa)	$E_{sec1/3}$ (Kpa)	$E_{sec1/2}$ (Mpa)	$E_{sec1/3}$ (Mpa)
266471.35	0.9104	145163.45	185599.42	91.63	114.68
77223.28	0.6469	52243.191	60569.885		
138664.27	0.8820	77510.41	97895.031		

3. RESULTS OF OUR APPROACH

We present here four categories of results. The first concerns results of soil identification tests (D_{max}, $PI, D_{50}, f, G, S, L, A$) as well as the elastic-plastic parameters (Table 6); the second category of results represents the values of Young moduli calculated based on multiple correlations with soil identification parameters (Table 7). There will therefore be E_{LCPC} calculated with the first correlation and the E_{SIKALI} calculated with the second. The third category of results relates to the Young's moduli values deduced from triaxial test results based on the hyperbolic model of Duncan and Wong (Table 8).

We will have:

E_t^0:initial tangent modulus,

E_{elq}:The equivalent modulus,

$E_{sec1/3}\ et\ E_{sec1/2}$: The secant moduli.

The results of the fourth category allow us to estimate the correspondence between the two categories of Young's moduli values, we have drawn the lines of linear regressions and calculated the correlation coefficients between each value of the second and third group. The figures 9 to 16 and the tables 9 to10 summarize the expressions of straight linear regressions obtained and table 11 highlights the most relevant matches.

Table 6 Identification of soil parameters

Sites	N°	Name	D_{max}(mm)	D_{50}(mm)	PI(%)	G(%)	S(%)	L(%)	A (%)	C'(bars)	ϕ'(degree)
BINI A WARAK	1	PG101	20	2.5	29.3	49.25	29.28	6.38	14.11	0.23	27.1
	2	PG102	10	4.5	38.6	49.56	17.05	15.94	17.45	0.15	32
	3	PG103a	12.5	0.4	20	41.49	34.19	8.57	15.75	0.49	30.9
	4	PG103b	10	2	20	38.61	30.78	14.55	16.06	0.53	21.1
	5	PG104a	10	0.7	19.7	33.81	47.16	7.98	11.05	0.08	35.4
	6	PG104b	15	9	15.1	40.365	30.825	11.585	17.225	0.13	34.9
	7	PD101a	12.5	2.6	22.4	55	27.37	6.35	11.21	0.17	32.1
	8	PD101b	10	2.5	30	46.18	27.95	7.44	11	0.38	27.9
	9	PD102	10	0.5	20.5	36.99	31.2	16.81	15	0.1	30.5
	10	PD103a	12.5	7.5	22	60.79	16.99	13.21	9.01	0.03	37.3
	11	PD103b	15	4	15.1	40.37	30.83	11.59	15.23	0.45	28
LOM PANGAR	12	PG101	12.5	0.005	13	35	25	20	20	0.36	28
	13	PG102	10	0.01	14	45	21	19	15	0.36	29
	14	PG103a	12.5	0.5	15	45	22	13	20	0.31	39
	15	PG103b	15	0.045	29	35	33	10	22	0.4	31
	16	PG104a	12.5	0.012	21	46	26	10	18	0.28	37
	17	PG104b	12.5	0.0675	20	32	28	21	19	0.75	30
	18	PD101a	5	0.29	25	35	32.5	21	11.5	0.32	34
	19	PD101b	15	0.29	25	31	29	25	15	0.09	21
	20	PD102	12.5	0.014	19	33	20	25	20	0.28	33
	21	PD103a	10	0.05	25	36	30	19	15	0.38	33
	22	PD103b	15	1.2857143	34	35	25	3	37	0.5	29
	23	PD104a	12.5	0.017	14	36	27	19	18	0.16	32
	24	PD104b	12.5	0.022	15	34	32	14	20	0.45	30
	25	PEG204b	12.5	4.8	20	27	31	12	30	0.2	35
	26	PED303a	15	0.01	14	47	25	13	15	0.75	30

Table 7 Young's moduli values calculated on the basis of the correlations

Sites	N°	Calculated Young's moduli	
		E_{LCPC} (MPa)	E_{SIKALI} (MPa)
BINI A WARAK	1	153.26	81.34
	2	63.05	38.21
	3	94.15	52.36
	4	84.49	49.85
	5	90.95	50.32
	6	149.68	87.61
	7	118.71	66.69
	8	81.711	46.78
	9	76.64	43.46
	10	129.91	73.04
	11	145.56	82.73
LOM PANGAR	12	62.57	33.21
	13	60.17	32.52
	14	88.62	51.92
	15	68.70	36.53
	16	64.22	34.08
	17	68.45	37.21
	18	39.20	23.36
	19	93.14	48.68
	20	53.94	29.05
	21	58.74	31.60
	22	54.82	34.57
	23	72.66	38.80
	24	70.64	38.28
	25	74.22	46.84
	26	93.37	47.48

Table 8 Values of the Young'smoduli inferred from the results of the triaxial test

Sites	N°	Experimental moduli			
		E_t^0(MPa)	E_{elq}(MPa)	$E_{sec1/2}$(MPa)	$E_{sec1/3}$(MPa)
BINI A WARAK	1	160.79	173.48	91.63	114.68
	2	49.67	82.62	30.58	36.95
	3	93.67	99.25	53.28	66.752
	4	66.34	77	46.72	53.26
	5	73.06	80.88	46.97	55.67
	6	159.19	169.58	89.41	112.67
	7	113.16	115.13	65.92	81.66
	8	90.38	97.58	55.39	67.06
	9	73.16	68.64	46.93	55.67
	10	137.96	147.26	77.75	97.82
	11	153.33	168.43	83.35	106.68
LOM PANGAR	12	59.52	56.042	32.94	40.64
	13	59.06	62.19	39.21	44.43
	14	77.39	78.51	16.39	19.29
	15	224.88	226.93	118.56	154.00
	16	79.13	61.81	24.93	27.67

	17	62.62	63.14	24.93	27.67
	18	43.76	40.95	28.24	32.47
	19	97.67	89.21	67.22	74.55
	20	99.40	100.07	68.36	78.71
	21	66.99	58.33	31.88	36.14
	22	324.06	285.15	153.35	197.29
	23	89.16	91.2	58.24	68.55
	24	138.5	139.17	75.08	96.22
	25	64.06	67.97	37.01	47.14
	26	67.973	120.83	42.89	51.25

Analysis of the scattered values between experimental and calculated moduli highlights the presence of two outliers that were eliminated following the recommendations of the analytical statistics. We then traced the curves trends on the remaining scattered values. These trends curves are based on the least squares method (linear model).

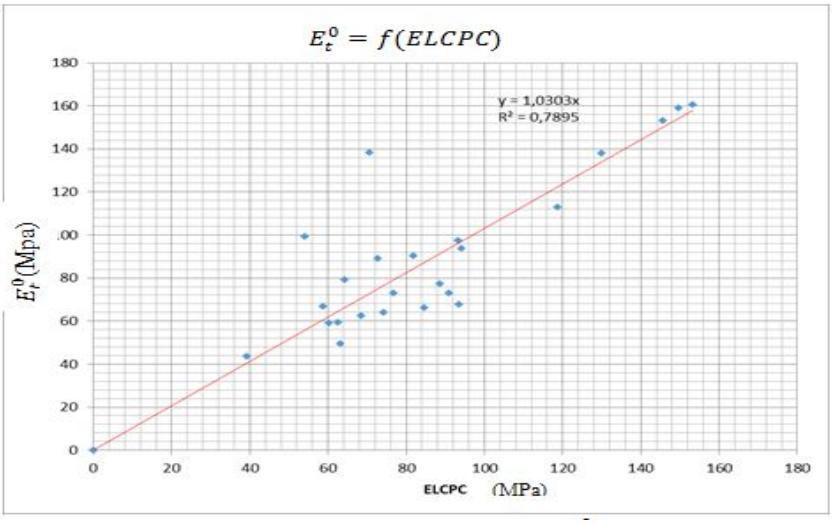

Figure 9 Trend curve between E_t^0 and E_{LCPC}

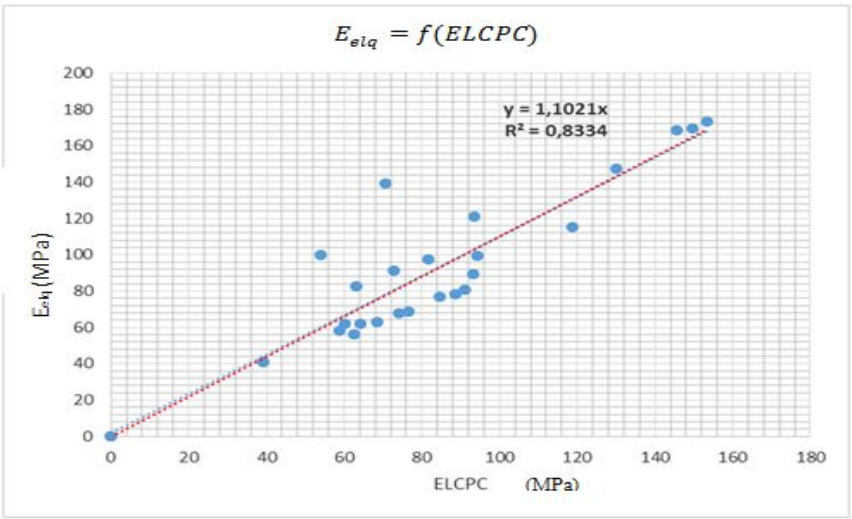

Figure 10 Trend curve between E_{elq} and E_{LCPC}

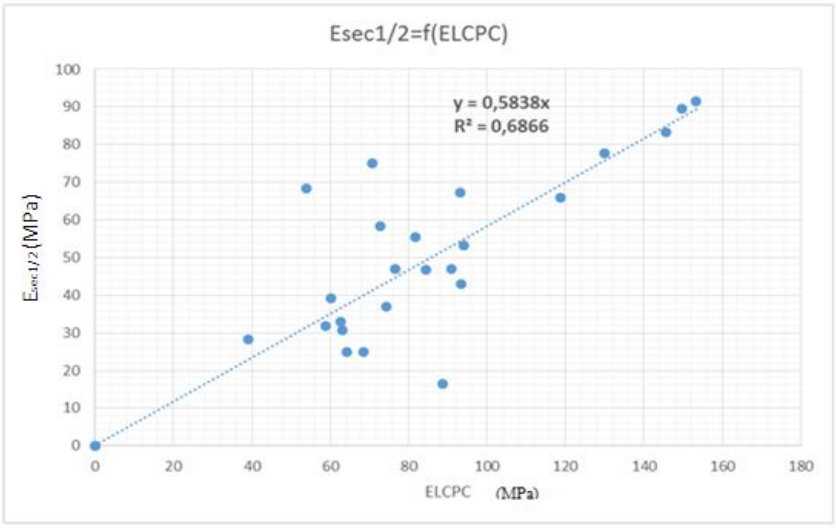

Figure 11 Trend curve between $E_{sec1/2}$ and E_{LCPC}

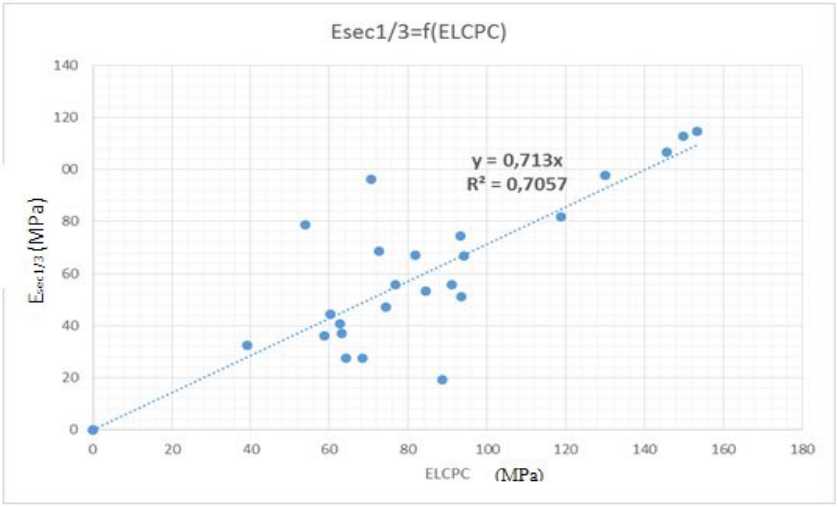

Figure 12 Trend curve between $E_{sec1/3}$ and E_{LCPC}

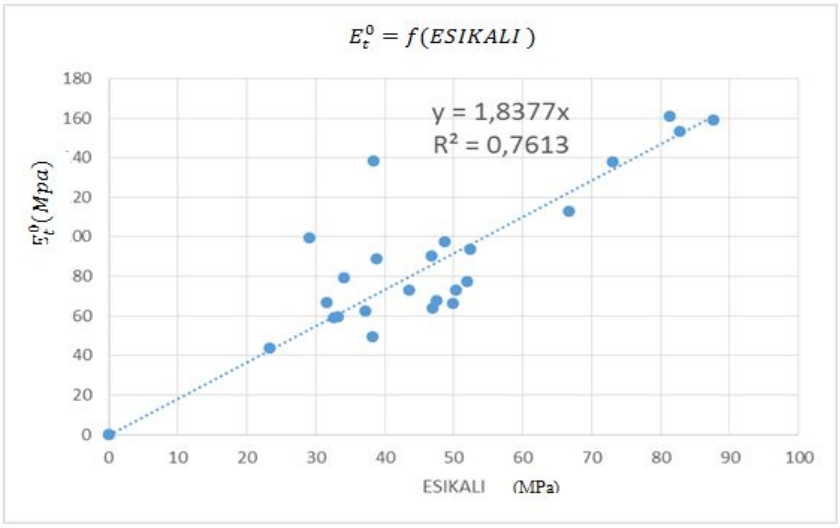

Figure 13 Trend curve between $E_t^0$and E_{SIKALI}

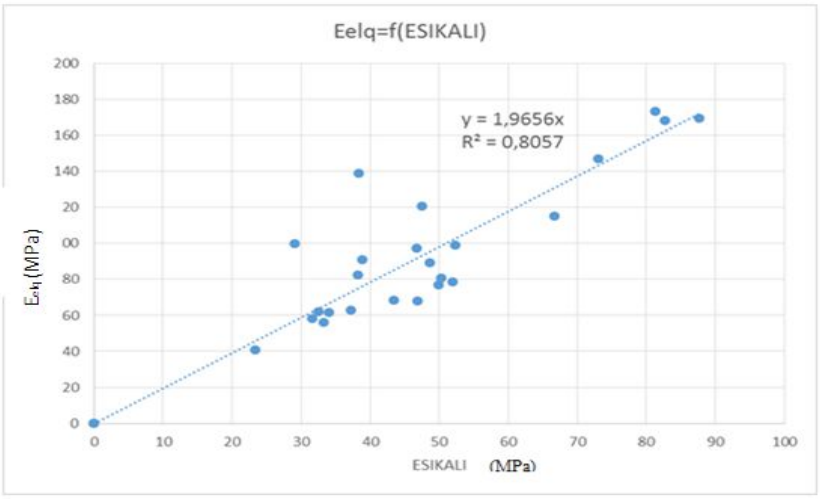

Figure 14 Trend curve between E_{elq} and E_{SIKALI}

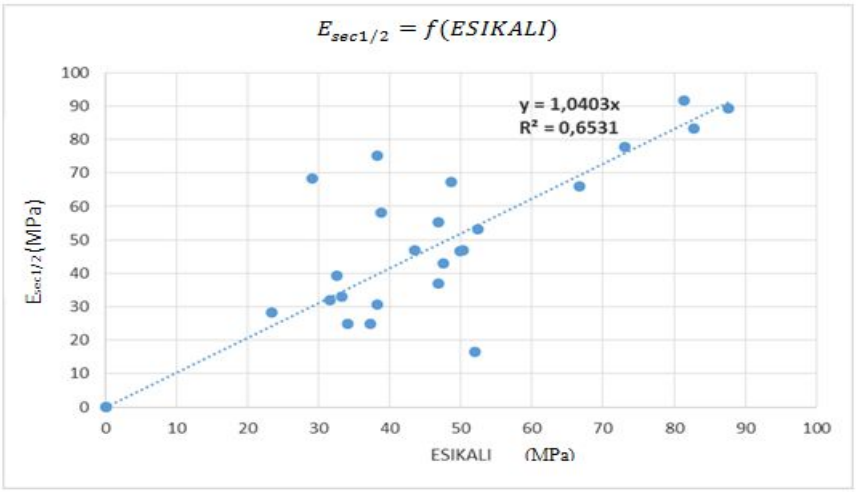

Figure 15 Trend curve between $E_{sec1/2}$ and E_{SIKALI}

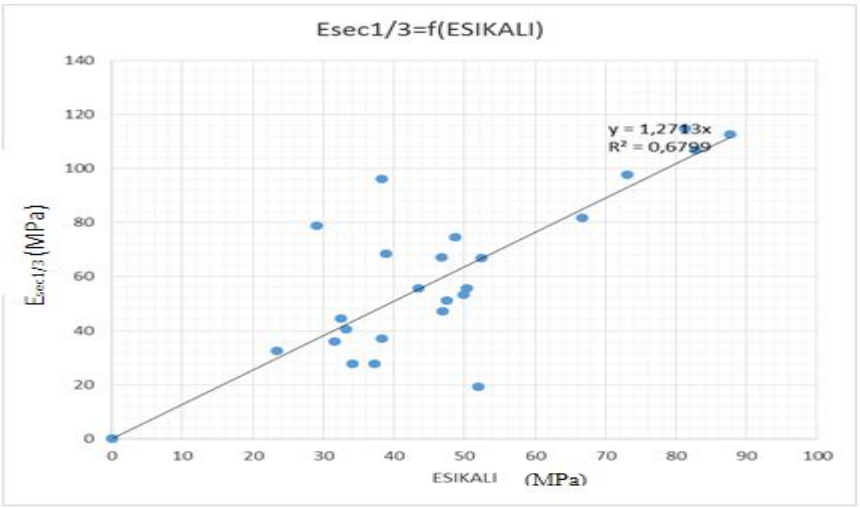

Figure 16 Trend curve between $E_{sec1/3}$ and E_{SIKALI}

Table 9 Summary of the regression lines depending on E_{LCPC}

Young modulus	Linear regressions	R-Square values
$E_t^0 = f(ELCPC)$	$y = 1.0303x$	R²=0.7895
$E_{elq} = f(ELCPC)$	$y = 1.1021x$	R²=0.8334
$E_{sec1/2} = f(ELCPC)$	$y = 0.5838x$	R²=0.6866
$E_{sec1/2} = f(ELCPC)$	$y = 0.713x$	R²=0.7057

Table 10 Summary of the regression lines depending on E_{SIKALI}

Young modulus	Linear regressions	R-Square values
$E_t^0 = f(ESIKALI)$	$y = 1.8377x$	R²=0.7613
$E_{elq} = f(ESIKALI)$	$y = 1.9656x$	R²=0.8057
$E_{sec1/2} = f(ESIKALI)$	$y = 1.0403x$	R²=0.6531
$E_{sec1/2} = f(ESIKALI)$	$y = 1.2713x$	R²=0.6799

Table 11 Selected regression lines for our local data

Young modulus	Linear regressions	R-Square values
$E_t^0 = f(ELCPC)$	$y = 1.0303x$	R²=0.7895
$E_{elq} = f(ELCPC)$	$y = 1.1021x$	R²=0.8334
$E_{sec1/2} = f(ESIKALI)$	$y = 1.0403x$	R²=0.6531

4. CONCLUSION

For pavement design some authors use the initial tangent modulus, others the secant moduli at predetermined points. The theory of soil mechanics defines several Young's moduli and empirical calculation formulas of these parameters do not often specify the nature of the modulus. Then it is important to specify the nature of the Young's modulus that our correlations describe through the evaluation of the regression lines between calculated and measured values (Table 9 and 10).This evaluation between estimated and calculated Young modulus has been obtained with our collected samples and the regression equations have provided significative results with a high R-Square value (Table 11). We saw that the LCPC modulus is closer to the initial tangent modulus and the equivalent modulus. The Sikali modulus approaches the secant modulus at 50% of the breaking stress. However, considering the number the relatively small samples, these results need to be confirmed or disproved by expanding further bank data necessary for the pursuit of this study.

5. ACKNOWLEDGEMENTS

We would like to thank the African Center of Excellence in Information and Communication technologies of University of Yaounde I for their collaboration and support.

REFERENCES

[1] Araft Johnson J. M., Bathia W. S. *Engineering properties of lateric soils*. Procedings of the 7th international conference, Mexico, vol.2, 1969, pp13-47.

[2] Behpoor L., Ghahranian A. Correlation of SPT to strength and modulus of elasticity of cohesive soils. Civil Engineering Department, Shiraz University, Shiraz, Iran, 1970, pp. 175-178.

[3] BohiZondje P. B. Caractérisation des sols latéritiques utilisés en construction routière : le cas de la région de l'Agneby (Côte d' Ivoire). PhD thesis, Ecole Nationale des Ponts et Chaussées, France, 2008.

[4] Cisse I. Problématique du choix du module des matériaux recyclés dans le dimensionnement par la méthode rationnelle : Application au tronçon Diamniadio-Mbour. Master Thesis, Ecole Polytechnique, Thies, Senegal, 2003.

[5] Dano C., Hicher P.Y., Benazzong I.K., Le Touzo J.Y., une cellule triaxiale de grande taille pour l'étude du comportement des sols. Revue de l'Institut de Recherche en Genie Civil et Mecanique, Ecole Centrale de Nantes, Université de Nantes, CNRS, pp. 1-8.

[6] FallM. Note sur les matériaux latéritiques et quelques résultats sur les latéritiques du Senegal. PhD Thesis, Institut National Polytechnique de Naney, France, 1993.

[7] Jauve P., Milaud E. Application des modèles non linéaires au calcul des chaussées souples. *Bulletin de liaison du laboratoire des ponts et chaussées*, N° 190, France, 1994, pp. 39-55.

[8] Laboratoire Central des Ponts et Chaussées. Dimensionnement des chaussées, Paris, 2003.

[9] Ladjal S. Modelisation des non linearités de comportement des sols fins sous sollicitations homogènes : application à la simulation des résultats d'essais triaxiaux classiques. Master thesis, Université Mohamed Boudiaz de M'Sila, Algerie, 2004.

[10] Le Tirant P. Appareil triaxial pour étude des sols fins : description et mise au point. *Bulletin de liaison du laboratoire des ponts et chaussées*, N° 69, France, 1964, pp. 7-12.

[11] Magnan J.P. Lois de comportement et modélisation des sols. Laboratoire Central des Ponts et Chaussées France, 1997.

[12] Magnan J. P. Corrélations entre les propriétés des sols. Laboratoire Central des Ponts et Chaussées, France, 1998.

[13] Messi Alfred. F., Mamba Mpele.,Tchoumi Dany. F., KoumbeMbock., Okpwe. Mbarga.R. Multiples Correlations between physical properties of lateritic soils for pavement design. *International Journal of Civil Engineering and Technology*, volume 7, issue 5, September-October 2016, pp. 485-499.

[14] Mestat P., Reiffstak P. Modules de déformation en mécanique des sols : Définitions, détermination à partir des essais triaxiaux et incertitudes. Laboratoire central des Ponts et Chaussées, Paris, France, 2002.

[15] Mpeck J. E. Corrélations multiples entre les paramètres d'identification des laterites et les valeurs du coefficient de poisson et du module de Young, Master thesis, National Advanced School of Engineering, Yaoundé, Cameroon, 2012.

[16] Nguyen P.P.T. Etudes en place et en laboratoire du comportement en petites déformations des sols argileux naturels. PhD thesis, Ecole Nationale des Ponts et Chaussées, France, 2008.

[17] Putri E.E., Rao N.S.V.K., Mannan A. Evaluation of the modulus of elasticity and resilient modulus for Highway subgrades. EJGE. University Malaysia Sabah, Kota Hinabalu, Malaysia, 2010, pp. 1285-1293.

[18] Reiffstak P., Tacita J.L., Mestat P., Pilniere F. La presse triaxiale pour éprouvettes cylindriques creuses au LCPC adaptée à l'étude des sols naturels. *Bulletin de liaison du laboratoire des ponts et chaussées*, N° 270-271, France, 2007, pp. 109-131.

[19] Sall I. Etude de la corrélation entre le module d'élasticité et l'indice portance CBR dans le dimensionnement des superstructures routières. Master thesis, Ecole Polytechnique,Senegal, 1990.

[20] Setra-LCPC. Conception et dimensionnement des structures de chaussées. Guide technique LCPC, 1996.

[21] Sikali F., Djalal M. E. Utilisateur des latérites en technique routière au Cameroun. National Advanced School of Engineering, Cameroon, 1981.

[22] Tchoumi D. F. corrélations multiples entre les paramètres d'identification d'un sol et ses paramètres de performance. Master thesis, National Advanced School of Engineering, Cameroon, 2016.

[23] Vu N.H., Rangeard D. Martinez J. Identification discrète des paramètres élastoplastiques des sols pulvérulents à partir de essais triaxial et préssiometrique. EA 3913, Institut National des Sciences Appliquées de RENNES, France, 2006.

[24] Ze B. R. Corrélations multiples entre les paramètres d'identification des graves concassés et leurs modules de Young. Master thesis, National Advanced School of Engineering, Cameroon, 2012.

[25] Zohou M. Etude de la corrélation entre les modules d'élasticité et l'indice de portance CBR dans le dimensionnement des superstructures routières. Application aux graveleux latéritiques, Master Thesis, Ecole Polytechnique, Thies, Senegal, 1991.

[26] Anand. Ayyagari, Srinivasa Rao.Kraleti and Lakshminarayana. Jayanti, Determination of Optimal Design Parameters For Control Chartw ith Truncated Weibull in-Control Times, *International Journal of Production Technology and Management (IJPTM),* 7 (1), 2016, pp. 1–17.

[27] Chandra Shekar, N B D Pattar and Y Vijaya Kumar, Design and Study of the Effect of Multiple Machining Parameters in Turning of AL6063T6 Using Taguchi Method. *International Journal of Design and Manufacturing Technology* 7(3), 2016, pp. 12–18.